

## Search for Higgs Particles in MSSM SUSY

---

**Christian Veelken\***

On behalf of the CMS Collaboration

*Laboratoire Leprince-Ringuet, École Polytechnique, 91128 Palaiseau, France*

*E-mail: [christian.veelken@cern.ch](mailto:christian.veelken@cern.ch)*

A search for charged and neutral Higgs boson production in the context of the minimal supersymmetric standard model is presented. The search is based on proton–proton collision data recorded at  $\sqrt{s} = 7$  TeV center–of–mass energy by the CMS experiment in 2011. The production of charged Higgs bosons is analyzed in the decay channel to tau lepton and neutrino. The presence of neutral Higgs bosons in the CMS data is tested in three channels: in decays to pairs of bottom quarks, taus and muons. The analyzed dataset corresponds to an integrated luminosity of 2.0–5.0 fb<sup>-1</sup>, depending on analysis channel.

*36th International Conference on High Energy Physics,  
July 4-11, 2012  
Melbourne, Australia*

---

\*Speaker.

## 1. Introduction

The minimal supersymmetric standard model (MSSM) predicts the existence of five elementary Higgs particles: two CP–even ( $h$ ,  $H$ ), one CP–odd ( $A$ ) plus two charged ( $H^+$ ,  $H^-$ ) bosons. Neutral MSSM Higgs bosons may be produced via two production processes: gluon–gluon fusion ( $gg \rightarrow \Phi$ ) and  $b\bar{b}$  annihilation ( $b\bar{b} \rightarrow \Phi$ ). In the latter case there is a significant probability to observe a  $b$ –quark jet in association with the Higgs boson in the detector.

A search for neutral and charged Higgs particles in the proton–proton collision data recorded by the CMS experiment in 2011 is presented. Charged Higgs bosons in the mass range  $M_{H^\pm} < m_{top}$  are searched for via their decays into tau lepton plus neutrino. The production of neutral Higgs bosons is studied in three channels: in decays to bottom quark, tau and muon pairs. The analyzed dataset has been recorded at a center–of–mass energy of  $\sqrt{s} = 7$  TeV and corresponds to an integrated luminosity of 2.0–5.0 fb $^{-1}$ , depending on analysis channel.

## 2. Detector and reconstruction

The CMS detector is described in detail elsewhere [1]. The central feature of the CMS apparatus is a superconducting coil of 6 m diameter, providing a field of 3.8 T. The tracking detector, located at the center, is built from silicon pixel plus strip modules and measures the momenta of charged particles within the pseudo–rapidity range  $|\eta| < 2.5$ . The energy of particles within  $|\eta| < 3.0$  is measured by a lead tungstate crystal electromagnetic plus brass–scintillator hadronic calorimeter, which surround the tracking detector. Gas–ionization detectors embedded in the steel return yoke of the solenoid reconstruct muons within  $|\eta| < 2.5$ . Forward calorimetry extends the geometric acceptance of the detector up to  $|\eta| < 5.0$ .

A particle–flow (PF) algorithm [2] is used to combine the information from all subdetectors and reconstruct electrons, photons, muons, charged and neutral hadrons. Hadronic tau decays, denoted by  $\tau_{had}$ , are reconstructed by the HPS algorithm [3], based on the collection of charged and neutral hadrons. Jets are reconstructed using the anti– $k_T$  algorithm with a distance parameter of  $R = 0.5$ . Jets originating from hadronization of bottom quarks within the acceptance of the tracking detector are identified using algorithms based on impact parameters of tracks with respect to the event vertex and reconstruction of  $b$ –hadron decay vertices. The missing transverse momentum,  $\cancel{E}_T$ , is computed by summing the momenta of all particles reconstructed by the PF algorithm.

## 3. Search for charged Higgs bosons

Charged MSSM Higgs bosons,  $H^{\pm 1}$ , of mass  $m_{H^\pm} < (m_t - m_b)$  are searched for in top quark decays. For values of  $\tan\beta > 5$  the charged Higgs boson predominantly decays into taus, altering the tau lepton yield in  $t\bar{t}$  events compared to the standard model (SM).

Three different final states are studied [4]:  $\tau_{had} + \text{jets}$ ,  $\tau_{had} + \ell$  ( $\ell = e$  or  $\mu$ ) and  $e + \mu$ . Events in the  $\tau_{had} + \text{jets}$  final state are selected by requiring the presence of a  $\tau_{had}$  of  $P_T > 40$  GeV and  $|\eta| < 2.3$ , plus three jets of  $P_T > 30$  GeV, at least one of which is required to be  $b$ –tagged. Contribution of QCD multi–jet background to the  $\tau_{had} + \text{jets}$  channel is removed by requiring  $\cancel{E}_T > 50$  GeV and  $\Delta\phi(\tau_{had}, \cancel{E}_T) < 160^\circ$ .  $\tau_{had} + e$  ( $\tau_{had} + \mu$ ) candidate events are selected by requiring a  $\tau_{had}$  of

<sup>1</sup>We use the symbol  $H^{\pm}$  to refer to Higgs bosons of positive as well as of negative charge.

$P_T > 20$  GeV and  $|\eta| < 2.3$ , two jets of  $P_T > 35$  GeV (first) and  $P_T > 30$  GeV (second) plus an isolated electron of  $P_T > 35$  GeV,  $|\eta| < 2.5$  (isolated muon of  $P_T > 30$  GeV,  $|\eta| < 2.1$ ) and charge opposite to  $\tau_{had}$ . At least one of the jets is required to pass b-tag discriminators. Background contributions to the  $\tau_{had} + e$  ( $\tau_{had} + \mu$ ) channel are suppressed by a  $\cancel{E}_T > 45$  GeV ( $\cancel{E}_T > 40$  GeV) cut. Events in the  $e + \mu$  channel are required to contain an isolated electron of  $P_T > 20$  GeV and  $|\eta| < 2.1$ , an isolation muon of  $P_T > 20$  GeV and  $|\eta| < 2.4$  plus two jets of  $P_T > 30$  GeV.

The number of events observed in the data is in agreement with the SM expectation. The analyzed dataset corresponds to an integrated luminosity of  $\mathcal{L} = 2.0\text{--}2.3$  fb $^{-1}$ . The background arising from jet  $\rightarrow \tau_{had}$  fakes is estimated using control regions in data. Contributions of other background processes are obtained from Monte Carlo simulation.

An upper limit on the branching fraction  $\mathcal{B}(t \rightarrow H^+ b)$  is set, assuming  $\mathcal{B}(H^+ \rightarrow \tau \nu) = 100\%$ . The limit is computed via the  $CL_s$  method [5]. The input to the limit computation are: in the  $\tau_{had} + \ell$  and  $e + \mu$  channel the number of observed and expected events and in the  $\tau_{had} + \text{jets}$  channel the observed and expected distribution of the  $\tau_{had} + \cancel{E}_T$  transverse mass. The result is shown in Fig. 1, together with the corresponding region in MSSM  $m_{H^+} - \tan \beta$  parameter space excluded by the CMS search for charged MSSM Higgs bosons.

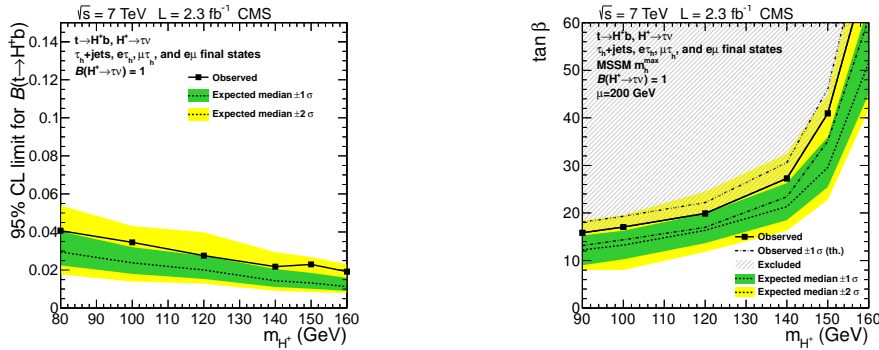


**Figure 1:** Left: Upper limit on  $\mathcal{B}(t \rightarrow H^+ b)$  as function of  $m_{H^+}$ . Right: Region in  $m_{H^+} - \tan \beta$  parameter space excluded by the CMS search for  $H^+ \rightarrow \tau \nu$ . Branching fractions  $\mathcal{B}(t \rightarrow H^+ b)$  as function of  $m_{H^+}$  and  $\tan \beta$  have been computed for the  $m_h^{max}$  scenario [6] of the MSSM.

#### 4. Search for neutral Higgs bosons

The production of neutral MSSM Higgs bosons is studied in three complementary channels:  $\Phi \rightarrow b\bar{b}$ ,  $\Phi \rightarrow \tau^+ \tau^-$  and  $\Phi \rightarrow \mu^+ \mu^-$ <sup>2</sup>. The decay into  $b\bar{b}$  provides the largest branching fraction, but suffers from an overwhelmingly large background of QCD multi-jet production. The branching fraction for the decay into  $\tau^+ \tau^-$  is about one order of magnitude lower. The presence of two electrons, muons or hadronically decaying taus in the event provides a much improved signal to background ratio compared to the  $b\bar{b}$  decay mode, however. The decay into  $\mu^+ \mu^-$  has a branching fraction of  $10^{-4}$ – $10^{-3}$ . The advantages of this decay mode are the low level of backgrounds, high reconstruction efficiency for muons plus excellent mass resolution.

<sup>2</sup>We denote by  $\Phi$  the sum of scalar and pseudo-scalar Higgs bosons,  $h$ ,  $H$  and  $A$ , as appropriate.

#### 4.1 $\Phi \rightarrow \tau^+ \tau^-$

The search for  $\Phi \rightarrow \tau^+ \tau^-$  is performed in three final states [7]:  $\tau_{had} + e$ ,  $\tau_{had} + \mu$  and  $e + \mu$ . Events in the  $e + \mu$  channel are selected by requiring an isolated electron of  $P_T > 10$  GeV and  $|\eta| < 2.3$  plus an isolated muon of opposite charge, satisfying  $P_T > 10$  GeV and  $|\eta| < 2.1$ . Trigger conditions require that either one of the two leptons passes  $P_T > 20$  GeV. In the  $\tau_{had} + e$  ( $\tau_{had} + \mu$ ) channel an isolated electron (muon) of  $P_T > 20$  GeV and  $|\eta| < 2.1$  is required, plus a  $\tau_{had}$  of opposite charge,  $P_T > 20$  GeV and  $|\eta| < 2.3$ . In all final states  $W$ +jets and  $t\bar{t}$  backgrounds are reduced by requiring the reconstructed  $\cancel{E}_T$  to point in direction of the visible tau decay products. Events with additional leptons are rejected to suppress  $Z/\gamma^* \rightarrow e^+e^-$  and  $Z/\gamma^* \rightarrow \mu^+\mu^-$  backgrounds.

The statistical analysis is performed in two distinct event categories in order to enhance the sensitivity of the search: Events in the first category are required to contain a b-tagged jet of  $P_T > 20$  GeV and  $|\eta| < 2.4$ . Events without such jet enter the second category.

The event yields observed in all categories and final states, in a dataset corresponding to an integrated luminosity of  $\mathcal{L} = 4.6 \text{ fb}^{-1}$ , are compatible with the background expectation. Contributions of QCD multi-jet,  $W$  + jets and the dominant irreducible  $Z \rightarrow \tau^+ \tau^-$  background are determined using data, predictions for other background processes are obtained from Monte Carlo simulation.

The mass of tau-pairs,  $M_{\tau\tau}$ , is reconstructed with a resolution of typically 20%, using an algorithm developed by CMS [8]. The distribution of  $M_{\tau\tau}$  in events selected in the combination of  $\tau_{had} + e$ ,  $\tau_{had} + \mu$  and  $e + \mu$  final states is shown in Fig. 2. The distributions observed in both event categories are in agreement with the expectation for SM background processes.

The observed distributions of  $M_{\tau\tau}$  are used to set an upper limit on the signal contribution to the data. The region in MSSM parameter space excluded by the CMS search for  $\Phi \rightarrow \tau^+ \tau^-$  is shown in Fig. 2.

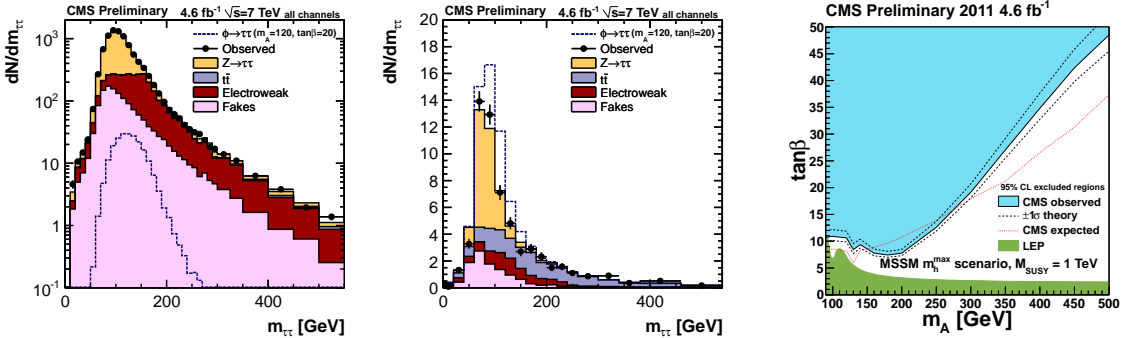


**Figure 2:** Left and center: Distribution of tau-pair mass  $M_{\tau\tau}$  reconstructed in  $\Phi \rightarrow \tau^+ \tau^-$  candidate events with zero (left) and one (center) b-tagged jet, selected in any of the decay modes  $e\mu$ ,  $e\tau_{had}$  and  $\mu\tau_{had}$ . The expected signal assuming  $M_A = 120$  GeV and  $\tan\beta = 20$  is shown for comparison. Right: Region in  $m_A$ - $\tan\beta$  parameter space excluded by the CMS search for  $\Phi \rightarrow \tau^+ \tau^-$ . The exclusion contour has been computed for the  $m_h^{max}$  scenario [6] of the MSSM.

#### 4.2 $\Phi \rightarrow b\bar{b}$

The search for  $\Phi \rightarrow b\bar{b}$  is performed in two channels: in events with three jets passing b-tag discriminators (hadronic channel) [9] and in events containing two b-tagged jets plus a third jet

containing a muon (semi-leptonic channel) [10]. The requirement of a third jet compatible with a bottom quark decay removes a large fraction of the overwhelming background arising from heavy flavor QCD multi-jet production.

The selection of events in the hadronic channel is split into a low mass ( $M_\Phi < 180$  GeV) and high mass ( $M_\Phi > 180$  GeV) region. The leading and subleading jets are required to pass  $P_T > 46$  GeV (60 GeV) and  $P_T > 38$  GeV (53 GeV) in the low (high) mass analysis respectively. The thresholds are adapted to trigger requirements. The third jet is required to satisfy  $P_T > 20$  GeV in both mass regions. In the semi-leptonic channel, two jets of  $P_T > 30$  GeV plus one jet of  $P_T > 20$  GeV is required. Either the leading or the subleading jet is required to contain a muon of  $P_T > 15$  GeV.

An upper limit on the contribution of the  $\Phi \rightarrow b\bar{b}$  signal is set by a template fit of  $M_{bb}$ , the mass of leading plus subleading jet<sup>3</sup>. The corresponding exclusion region in MSSM parameter space is shown in Fig. 3. The analyzed dataset corresponds to an integrated luminosity of  $\mathcal{L} = 4.0$  fb<sup>-1</sup> (4.6 fb<sup>-1</sup>) in case of the hadronic (semi-leptonic) channel. In both channels the normalization and  $M_{bb}$  shape template for the dominant QCD multi-jet background are determined from data.

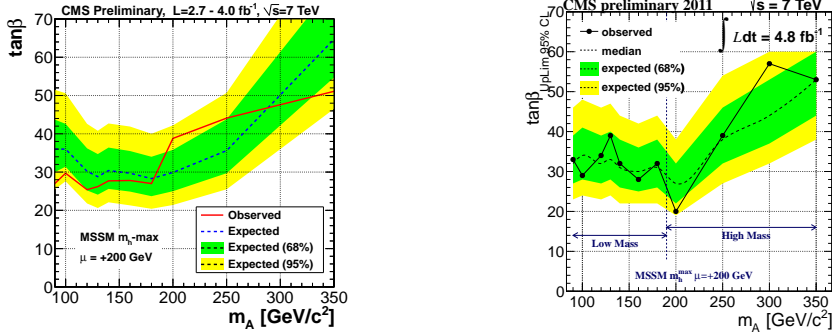


**Figure 3:** Region in  $m_A$ - $\tan\beta$  parameter space excluded by the CMS search for  $\Phi \rightarrow b\bar{b}$  in the hadronic (left) and semi-leptonic (right) channel. The exclusion contours have been computed for the  $m_h^{max}$  scenario [6].

#### 4.3 $\Phi \rightarrow \mu^+\mu^-$

Events in the  $\Phi \rightarrow \mu^+\mu^-$  channel are selected by requiring two isolated muons of opposite charge, of  $P_T > 30$  GeV for the leading and  $P_T > 20$  GeV for the subleading muon, within the pseudo-rapidity range  $|\eta| < 2.1$ . A  $\cancel{E}_T < 30$  GeV cut is applied to suppress  $t\bar{t}$  background.

Selected events are analyzed in three categories, designed to maximize the sensitivity of the search: Events in the first (second) category are required to contain a b-tagged jet of  $P_T > 20$  GeV and  $|\eta| < 2.1$  (to contain a third muon of  $P_T > 3$  GeV and  $|\eta| < 2.4$ ). Events which satisfy neither requirement enter the third category.

Drell-Yan muon pair production  $Z/\gamma^* \rightarrow \mu^+\mu^-$  constitutes the by far dominant background. The contribution of this irreducible background is estimated by fitting the distribution of the leading two muon mass,  $M_{\mu\mu}$ , in sidebands of the region where the signal is expected. The result of the fit is then extrapolated into the signal region.

<sup>3</sup>According to Monte Carlo simulations the two highest  $P_T$  jets originate from the Higgs decay in about 80% of signal events.  $M_{bb}$ , the mass of the two jets, is reconstructed with a resolution of typically 15%.

The distribution of  $M_{\mu\mu}$  observed in data is shown in Fig. 4. Note that the shape of a hypothetical signal exhibits two peaks: one representing the light scalar  $h$  and the other representing heavy scalar  $H$  plus pseudo-scalar  $A$  ( $m_A \sim m_H$  for the values of  $M_A$  and  $\tan\beta$  shown in the figure). The contribution of individual Higgs bosons can be resolved owing to the excellent mass resolution, amounting to about 2–3%, in this channel.

No evidence for a signal is observed in a dataset corresponding to an integrated luminosity of  $\mathcal{L} = 5.0 \text{ fb}^{-1}$ . The region in MSSM parameter space excluded by the CMS search for  $\Phi \rightarrow \mu^+\mu^-$  is shown in Fig. 4.

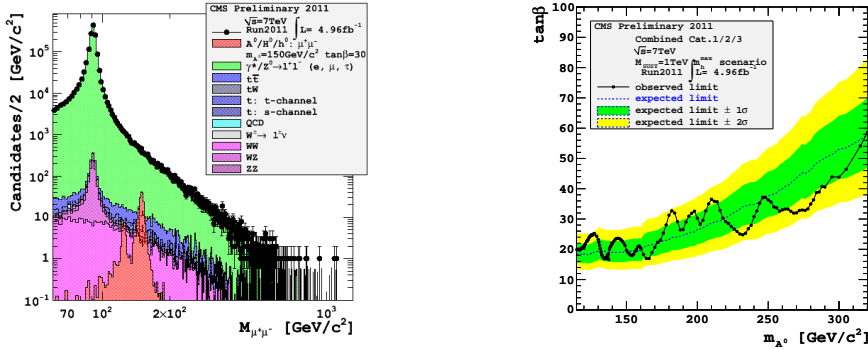


**Figure 4:** Left: Mass distribution of the muon pairs in  $\Phi \rightarrow \mu^+\mu^-$  candidate events. Right: Region in  $m_A$ - $\tan\beta$  parameter space excluded by the CMS search for  $\Phi \rightarrow \mu^+\mu^-$ .

## 5. Summary

The production of neutral and charged MSSM Higgs bosons in proton–proton collisions at  $\sqrt{s} = 7 \text{ TeV}$  has been studied using data recorded by the CMS experiment in 2011. No evidence for a signal is found in a dataset corresponding to an integrated luminosity of 2.0–5.0  $\text{fb}^{-1}$ . The non-observation of a signal excludes previously unexplored regions of MSSM parameter space.

## References

- [1] R. Adolphi *et al*, *JINST* **0803**, S08004 (2008).
- [2] CMS Collaboration, CMS-PAS-PFT-09-001, <http://cdsweb.cern.ch/record/1194487>.
- [3] CMS Collaboration, CMS-PAS-TAU-11-001, <http://cdsweb.cern.ch/record/1337004>.
- [4] CMS Collaboration, CMS-PAS-HIG-11-019, <http://cdsweb.cern.ch/record/1451606>.
- [5] T. Junk, *NIMA* **434**, 435 (1999); A. L. Read, CERN Yellow Report CERN-2000-005 (2000); ATLAS and CMS Collaborations, ATL-PHYS-PUB-2011-11, CMS Note-2011/005 (2011).
- [6] M. S. Carena *et al*, *Eur. Phys. J. C* **26**, 601 (2003); M. S. Carena *et al*, *Eur. Phys. J. C* **45**, 797 (2006).
- [7] CMS Collaboration, CMS-PAS-HIG-11-029, <http://cds.cern.ch/record/1406353>.
- [8] CMS Collaboration, *Phys. Lett. B* **716**, 30 (2012).
- [9] CMS Collaboration, CMS-PAS-HIG-12-026, <http://cdsweb.cern.ch/record/1460104>.
- [10] CMS Collaboration, CMS-PAS-HIG-12-027, <http://cdsweb.cern.ch/record/1460105>.
- [11] CMS Collaboration, CMS-PAS-HIG-12-011, <http://cdsweb.cern.ch/record/1453716>.